



Deposited via The University of Leeds.

White Rose Research Online URL for this paper:

<https://eprints.whiterose.ac.uk/id/eprint/89428/>

Version: Accepted Version

---

**Article:**

Antony, SJ, Chapman, D, Sujatha, SJ et al. (2015) Interplay between the inclusions of different sizes and their proximity to the wall boundaries on the nature of their stress distribution within the inclusions inside particulate packing. *Powder Technology*, 286. 98 - 106. ISSN: 0032-5910

<https://doi.org/10.1016/j.powtec.2015.08.007>

---

© 2015, Elsevier. Licensed under the Creative Commons Attribution-NonCommercial-NoDerivatives 4.0 International <http://creativecommons.org/licenses/by-nc-nd/4.0/>

**Reuse**

Items deposited in White Rose Research Online are protected by copyright, with all rights reserved unless indicated otherwise. They may be downloaded and/or printed for private study, or other acts as permitted by national copyright laws. The publisher or other rights holders may allow further reproduction and re-use of the full text version. This is indicated by the licence information on the White Rose Research Online record for the item.

**Takedown**

If you consider content in White Rose Research Online to be in breach of UK law, please notify us by emailing [eprints@whiterose.ac.uk](mailto:eprints@whiterose.ac.uk) including the URL of the record and the reason for the withdrawal request.

S. J. Antony\*, D. Chapman, J. Sujatha and T. Barakat (2015) ‘Interplay between the inclusions of different sizes and their proximity to the wall boundaries on the nature of their stress distribution within the inclusions inside particulate packing’, **Powder Technology**, 286, 98-106

**ACCEPTED Manuscript:**

**Interplay between the inclusions of different sizes and their proximity to the wall boundaries on the nature of their stress distribution within the inclusions inside particulate packing**

S. Joseph Antony<sup>1\*</sup>, David Chapman<sup>1</sup>, S. Jude Sujatha<sup>2</sup> and Thabit Barakat<sup>3</sup>

<sup>1</sup> *Institute of Particle Science and Engineering, School of Chemical and Process Engineering, University of Leeds, LS2 9JT, UK*

<sup>2</sup> *Department of Civil Engineering, University College of Engineering, Nagercoil, 629004, India*

<sup>3</sup> *Department of Physics and Astronomy, College of Science, King Saud University, PO Box 2455, Riyadh, Saudi Arabia*

**Abstract:** Micromechanical responses of granular materials are complex to understand when their behaviour is viewed in a single grain-scale. Experimental sensing of stresses within a grain-scale inside three dimensional particulate packing is still difficult to perform. In this work, photo stress analysis tomography (PSAT) is used to sense the fundamental nature of the stress experienced by different sizes of optically-sensitive inclusions inside granular packing (quasi-three dimensional) under an external axial-compression loading. The distribution of the maximum shear stress and the direction of the major principal stress experienced by the inclusions are analysed to understand the interplay between the size of the inclusions and their proximity to the wall boundary. The outcomes of this study provide a new understanding on the dual nature of stress transmission experienced by the inclusions, as

a result of the combined size and wall effects. Relatively large inclusions experience dominantly shear stress close to the wall boundaries while this nature tends towards hydrostatic away from the wall boundaries. Smaller size inclusions could experience shear at both close to and away from wall boundaries of the granular assembly. Computer simulations using three-dimensional discrete element method (DEM) are also performed to compare the qualitative nature of stress experienced by inclusions inside particulate media. Qualitatively, the simulation results also agree with the experimental outcomes, that an increase in the relative size of the inclusion decreases its ability to experience shear. Using DEM simulations, the fabric structure of the inclusions is examined in depth under mechanical loading. An increase in the size of the inclusions tends to decrease the fabric anisotropy of the contacts and in particular the strong contacts, surrounding them. Hence the micro scale origin of the weak mobilisation of shear in the large inclusions could be attributed to their relatively weak fabric anisotropy of the strong contacts surrounding them. These findings help to advance our understanding of the micromechanics of particulate systems, due to their size and proximity to wall boundaries: different sizes of the particles could sustain different nature of stresses within single-particle scale depending on their proximity to the wall boundaries.

Key words: Particulate mechanics, micromechanics, stress distribution, compaction, granular materials

\* Corresponding author: Email: S.J.Antony@leeds.ac.uk Ph.: 00441133432409

## **1. Introduction:**

Worldwide industries process a large proportion of feed stocks in granular and powder form. These include manufacturing ingredients of pharmaceutical tablets, food, cements, ceramics,

chemicals and energy materials. Micromechanical behaviour of granular materials, which is generally attributed to enlightening single-grain scale characteristics in granular assemblies and their links to bulk scale properties if any, is complex to understand [1]. Generally they differ from that of conventional states of matter viz., solid, liquid and gases, and often they possess their combined properties [1-3]. For example, a number of studies have focused on understanding the force transmission characteristics of granular materials under external loading environments [1-5]. It is widely recognised that the force-transmission inside granular assemblies occurs via inter-particle contacts in a non-homogeneous manner through a chain-like networks of contacts, often referred to as force chains [2-5]. Such observations have been made from photo elastic studies of birefringent grains [6-9], computer simulations using discrete element method (DEM) [10] and combined FEM-DEM [11]. For the granular materials, photo elastic studies were mostly reported for the two dimensional conditions whereas the DEM simulations accounted for both the two dimensional and three dimensional conditions [4, 10-13]. The link between the signature (structural alignment) of the force network and bulk mechanical properties of granular systems is quite significant [14]. For example, studies have attributed the microscopic origin of the bulk shear strength of granular materials, to the fabric alignment of the strong-force transmitting contacts under different external loading conditions [5,15,16]. Strong contacts account for a small proportion (about 25-30%) of all the contacts [2-5]. The strong contacts form the solid backbone to mobilise the shear strength, whereas the particles that share the weak contacts mostly account for the hydrostatic pressure (liquid-like behaviour) [2-5]. Similar to the force network, studies have also identified displacement networks in granular assemblies which account for their dilation and energy distribution characteristics [4].

In this work, we focus on the stress-transmission properties of inclusions in granular assemblies, with the emphasis being on the effects of their size and proximity to the wall boundaries when subjected to axial compressive loading. It is widely recognised that the size effects of particles could play a significant role on the compaction properties of granular assemblies [17]. In this case, size refers to the size distribution of the particles [18], relative size of particulate inclusions to their surrounding particles [19, 20] and sample size which in turn depends on the wall dimensions and the condition of the compressing chamber [21]. What is still lacking is clear information on how individual particles of different sizes, especially relatively big particles, distribute shear stress inside granular packing close to, and away from, the wall boundaries under external loading environments. This understanding is important, for example, in designing the size of functional active ingredients of pharmaceutical tablets [18, 22] and particulate composites [23]. This is also relevant for modelling particles more accurately in the DEM simulations. In the past, DEM simulations have been used for understanding the inter-particle interactions, the internal and macroscopic properties of granular assemblies under mechanical loading. However, they have not yet advanced to a level where the stress distribution characteristics *within* individual particles inside granular packing can be analysed easily. Conventional DEM simulations do not rigorously account for how stresses are distributed within individual particles [10,20,21]. In some FEM based simulation studies, individual grains were discretised into a large number of elements to predict stress distribution characteristics within the particles [1]. However due to the massive level of computing resources required to account for a large number of such particles in granular assemblies, using this methodology, information on the load transfer characteristics within single-particle scale inside granular assemblies is still not well established. Photo stress analysis tomography (PSAT) [8] has been applied to probe the stress distribution characteristics of inclusions in different surroundings. In these studies, a

known size of two dimensional inclusions (circular disk) was surrounded by three dimensional grains in such a way that the thickness of the inclusion and the grains were the same (quasi-3D experiments). Studies were performed using a number of positions for a single-size inclusion from the wall boundaries [8], or different sizes of inclusion positioned far away from walls [9] to sense the shear stress distribution experienced by the inclusion inside the granular assemblies under mechanical loading. They help to advance understandings on the stress distribution characteristics within single-particle scale. This aspect is generally difficult and computationally intensive, though not impossible to study using DEM simulations [10], especially when the size of the inclusion is much greater than the size of surrounding particles. In DEM, average stress calculations are based on inter-particle contact forces and, variations of stresses within particles, are not rigorously accounted for the stress calculations [10]. In the present work, we use PSAT methodology [8,9] to obtain insights on the interplay between the size effects of the inclusions and their proximity to wall boundaries, with an emphasis on the nature of stress distribution experienced by them inside granular assemblies subjected to axial compression.

## **2. Experiments**

### **2.1 Methodology:**

In the present study, experiments were conducted using PSAT [8] to measure the maximum shear stress and the direction of principal stresses at any points of interrogation on the birefringent inclusions. Detailed explanations on the working principles of photo stress analysis methodology for granular assemblies can be found elsewhere [24,25], however

briefly stated here. Basically, birefringent particles optically respond to stress when viewed under a circular polariscope setup [9,24,25]. Depending on the level of the induced stress, they display contours of fringes of different orders depending on the retardation of light passing through the fast and slow optical axes at the point of interest. Using the stress-optic law [25] the order of the fringes (retardation) can be related to the magnitude of the maximum shear stress  $\tau_{\max} (= (\sigma_{11}-\sigma_{33})/2$ , where  $\sigma_{11}$  and  $\sigma_{33}$  are the major and minor principal stress respectively). Also the direction of the principal stresses can be obtained anywhere on the birefringent inclusion by using a plane polariscope setup [25].

## **2.2 Experimental setup:**

Figure 1 shows the axial compression chamber made of glass in which a birefringent polymer disk (circular) inclusion with Young's Modulus 2.9MPa and Poisson's Ratio 0.4 was embedded in the middle of the particulate bed comprising of a uniformly sized 4mm diameter cohesionless and Vigna Radiata rigid beads (spheres) in random packing [8]. Initial packing density is  $0.73 \text{ g/cm}^3$ . The samples were prepared identically in all tests reported here, and follow a uniform protocol (layered filling of grains in random packing) and hence the tests repeatable [8]. This is verified by conducting the experiments three times for a given inclusion size. The nature of the stress distribution characteristics presented later in this paper was consistent in the multiple experiments for each case of the inclusion. The size ratio (SR) of the inclusion, which is the ratio between the diameters of the inclusion and the surrounding beads, was varied as 2.5, 4 and 7. The minimum size of the inclusion was kept to at least twice the size of the surrounding beads to ensure that the embedded inclusion was not trapped between the weak force chains (dead zones at micro scale) [2,4,5]. The thickness of the

inclusion disk is 4mm, which is also equal to the diameter of the surrounding matrix beads (quasi-3D condition). The inter-particle friction between the beads and beads-inclusion is 0.3. The wall boundaries were rigid and kept smooth as much as possible. The friction coefficient between the beads and wall material is about 0.006. The applied loading  $P$  pertains to quasi-static, uni-axial compression across the width of the bed (Fig.1).

To understand the combined effects of the size ratio of inclusions and wall effects, experiments were performed using different positions of inclusion from the wall boundaries represented in terms of  $\lambda d$  where  $\lambda$  varies between about 0-5 and  $d$  is the diameter of the inclusion (Fig.1). The inclusion is positioned at a fixed height from the loading pad. More details of the experimental compaction rig and protocol of testing used here can be found elsewhere [8]. Birefringent images for the distribution of maximum shear stress within sensor particles (inclusions) were recorded and analysed, both for the magnitude of maximum shear stress distribution and direction of the major principal stress within the sensor particles for different cases of the size ratio, loading level and position of the inclusion from the wall boundary within the granular bed.

### **3. Results and Discussions**

Profiles of the maximum shear stress distribution for different sizes of the inclusions in contact with the wall ( $\lambda=0$ ) for typical cases of compression load level ( $P$ ) is presented in Fig.2 below. The direction of the major principal stress distribution is also overlaid on the images. It is evident that the maximum shear stress distribution occurs in a non-homogeneous manner within the inclusions in contact with the wall. The extent of this non-homogeneity depends on the size of the particles. In the case of the lowest size ratio of the

inclusion (size ratio 2.5), the direction of the major principal stress within the inclusion mostly acts orthogonal to the direction of the applied loading. However, this trend changes to vertical direction (along the direction of axial compression) with an increase in the inclusion size. Under the uni-axial compression test (a form of strongly anisotropic external loading), the smallest size inclusion is capable of sustaining high levels of maximum shear stress, comparable to that of other large size inclusions. Increase in the inclusion size tends to transmit major principal stress along the direction of the compression loading. Hence the size of the inclusion tends to result a directional bias in transmitting the major principal stress, close to the wall boundaries, where shear field is expected to be more active.

Next, we examine an important nature of stress distribution experienced by the relatively large particles inside the granular assemblies which are subjected to compression. Previous studies on the size effects of the particles on their breakage [19,20,26] under mechanical loading have rather surprisingly reported that, relatively small size particles (and granules) tend to break rather than the large particles inside the particulate bed under mechanical loading. Such studies do not take into account the nature of stress distribution occurring within the particles, and this aspect is given attention in this paper. DEM simulations [20,27] on the mechanical behaviour of large particles inside granular assemblies (periodic boundary condition) subjected to tri-axial loading have revealed that solid particles experience liquid-like 'hydrostatic' state of stress (or negligible shear without directional bias) when their size ratio is greater than about 4. This hydrostatic dominance could retard their breakage. The reverse effect happens when their size ratio is less than 4 – i.e., the stress state was dominantly deviatoric (shear stress dominated, which is a measure of anisotropy in the stress transmitted) and less hydrostatic in nature. This shear dominated (anisotropic) behaviour of small particles could contribute to their breakage, relatively more, inside particulate packing

when other conditions are identical. This hypothesis has been backed by physical experiments, including testing the size effects of grain breakage under compression [27]. The experimental findings mostly agreed with this hypothesis although an exception was observed for a limited number of broken large particles residing close to the wall boundaries. This is possibly due to the wall effects in these experiments, although further studies are needed for the verification. Although the current PSAT experiments are not focused on studying the breakage behaviour of particles, in view of the above said context, it provides an opportunity to examine the nature of stress transmission experienced by the relatively large particles inside particulate beds. For example, from Fig.2 we could observe that for the largest inclusion (size ratio 7) in contact with the wall, it experiences a significant level of maximum shear stress ( $\tau_{\max}$ ) unlike if it were tested under periodic boundary condition [20]. This behaviour is analysed in detail and reported below.

Figure 3 shows the maximum shear stress distribution of the largest inclusion (size ratio 7) inside the granular assembly, for different distances  $\lambda d$  from the wall boundary ( $\lambda=0, 1, 2.67$  and 4.4) and under different levels of compressive loading. In this plot, the direction of the major principal stress experienced by the inclusions is also superimposed (dotted lines). When the largest inclusion is further away from the wall boundaries ( $\lambda=4.4$ ), the nature of stress experienced by it tends to be weak in shear, in spite of the strongly anisotropic axial boundary loading conditions and varying load levels tested here. This is also evident from the corresponding direction maps of the major principal stress, showing a relatively more homogenous distribution under different load levels (far right column of images in Fig.3). These observations for the case of the inclusion away from the wall boundaries agree with the results of previous DEM simulations of inclusions tested inside periodic cells [20]. Now it is

clear that the nature of stress distribution experienced by the relatively large inclusions is bi-modal depending on their proximity to wall boundaries: close to the wall boundaries it is shear stress dominated, whereas fairly away from the wall boundaries the shear stress intensity drops down significantly and the stress distribution tends to be more of hydrostatic nature.

Further we quantify the variation of maximum shear stress experienced within the inclusions, inside the granular bed, under external compressive loading. For this, we analysed the distribution of  $\tau_{\max}$  in the inclusions, averaged from data taken along four sections as illustrated in Fig.4. The results are presented in Figs. 5-7. From these plots, we could make some interesting observations. As shown in Figure 5, the inclusions (large and small) when in contact with the wall, experience a relatively significant level of shear. However, the position at which the highest value of maximum shear stress ( $\tau_{\max}$ ) occurs depends on the size of the inclusion. For the smallest size inclusion, this occurs relatively close to its boundary with a pronounced peak (and later we will show, at a distance predicted by the Hertzian theory). However, for the largest size inclusion, this occurs around the mid region of the inclusion. Hence, when an inclusion is in contact with the wall, it experiences a significant level of shear stress. This intensity decreases for an increase its proximity to the wall boundary. In general the above plots also show that shear stress distribution within single particle scale inside granular packing is not necessarily proportional to the applied load alone, but it also depends on the size of the particle.

From Figs.6-7 it is evident that the level of shear experienced by the inclusions tends to diminish when positioned away from the wall and more noticeably in the case of the largest

inclusion. However, what is most interesting is that the amount of shear experienced by the largest size inclusion is relatively low (Fig.7d) throughout the inclusion. This result, combined with the relatively more uniform distribution in the direction of major principal stress (Fig.3) when using the largest size inclusion, suggests that increase in the inclusion size tends to result in a relatively weak magnitude of shear stress distribution in them (and conversely tending towards the hydrostatic state) when they are present away from the wall boundaries (c.a. 4 times the size of the inclusion). Shear dominance of the inclusions, irrespective of their size, is clearly evident from the above presented results when positioned closer to the wall. The dual nature of shear experienced by the inclusions suggest that, in future it would be more appropriate to consider localised (wall) position-dependant and grain size-dependant descriptions of their shear strength in the theoretical constitutive modelling of granular materials under mechanical loading [28,29].

Further, we examine on the distance ( $Z_{\max}$ ) at which the peak value of maximum shear stress is experienced within the inclusions from their external boundary (surface). Fig.8 shows this for a typical case of inclusions in contact with the wall ( $\lambda=0$ ) under different load levels, normalized to half-width 'a' of the contact (Fig.4) obtained experimentally from image analysis. For simplicity, the data points in this plot are connected by a smoothing spline function for observing the general trends. The estimate of  $Z_{\max}$  based on the Hertian theory [30] is also shown as a dotted line for comparison.

It is evident that, in granular systems,  $Z_{\max}$  depends on the load intensity levels. We have also verified a similar trend in other positions of  $\lambda$  considered in this study. This implies that multiple interaction effects of contacts surrounding the grains influences the shear stress distribution characteristics within the inclusions. This aspect is usually not accounted in the

modelling of granular materials; for example DEM simulations for calculating the stress components of granular materials usually depend on the inter-particle contact forces only and not influenced by the interactions between neighbouring contacts [10] within the particles.

#### **4. Analysis of the fabric of the inclusions using DEM simulations**

Ideally, we would have liked to perform the above said experimental stress measurements in inclusions under three dimensional conditions. However such a task is very difficult to accomplish at present. Hence as presented earlier, quasi-three dimensional experiments were performed to understand the nature of stress distribution in the inclusions. However, in this section, we take advantage of the DEM simulations to probe the generic nature of stress distribution in the inclusions under three dimensional conditions. We show later that, indeed qualitative agreements are obtained. Then we take advantage of the simulations to potentially underline the role of the fabric alignment of contacts surrounding the inclusions to the nature of stress distribution within the inclusions to understand their micromechanical characteristics as presented below.

In particulate systems, the individual particles could move to a new position under external loading. Consequently their force distribution characteristics and the internal fabric could change and evolve depending on their particle-scale properties and loading environments [31]. Extensive levels of studies have been reported in the past, more fundamentally, on the role of internal fabrics of the particles on the micromechanical characteristics of particulate systems. For example, micromechanically based constitute relations are presented for sheared granular assemblies in which the evolution of different classes of contact fabric (e.g. in terms of contact normal) at grain scale are linked to macroscopic stress measures [5, 32-

34]. Hence, local constitutive relations can be prescribed in terms of the structural and kinematic variables of local scale, to understand how they contribute to mobilising macroscopic strength characteristics of granular materials. Several studies have been reported in the past on different types of the fabric measures in granular materials [35-37]. The distribution of the contact fabric and their correlation to the macroscopic stress tensor is also verified by photoelastic experiments, for example using birefringent rods of elliptical cross section subjected to simple shear [38,39] and pure shear [40]. A good level of correlation is reported between them. Such experimental responses were further integrated into the theoretical frameworks for describing the strength characteristics of granular materials [41-43]. These studies show that the local fabrics of the particles play a significant role in mobilising the mechanical strength characteristics of particulates at both micro and macro levels.

In the experimental work presented above, we have observed that the big particulate inclusions, when positioned away from wall boundaries, tend to experience shear relatively weakly for increase in their size. Therefore, to identify the underlying reason for this, it would be logical to investigate the fabric anisotropy of the inclusions in particulate packing subjected to mechanical loading. A detailed modelling of this aspect for all cases of the experiments performed here is computationally expensive, as well as outside the scope of the current work. However, as the size effects of the inclusions on the nature of stresses carried by them are more distinguishable when they are away from wall boundaries, here we present results from three-dimensional DEM simulations of a particulate bed (cuboidal) with a spherical inclusion at the centre of the bed subjected to tri-axial compression loading, for different sizes of the inclusions (Fig.9). The individual size of the surrounding particles (about 10000 spheres) is 100 $\mu$ m. The properties of all the particles are assigned as follows:

Young's modulus = 70 GPa, Poisson's ratio = 0.3, coefficient of inter-particle friction = 0.3, and interface energy =  $0.6 \text{ J m}^{-2}$ . Simulations were performed for different size ratio (SR=D/d, Fig.9) of the inclusion. In some cases, for comparison purposes, a mono-size particulate system was simulated (SR=1) under identical test conditions as before.

The particulate assembly is subjected to periodic boundary condition along its boundaries. Tri-axial compression loading (quasi-static) is applied and the assemblies are subjected to a constant mean stress (100kPa) test at all stages of loading ( $\sigma_{11} > \sigma_{22} = \sigma_{33}$ ) [34]. The axial strain was advanced in small increments of  $\Delta \varepsilon_{11} = 1.0 \times 10^{-5}$ , and several relaxation steps were performed within each increment to minimise the transient inertial effects that would have otherwise biased the results of a presumed quasi-static loading. The inter-particle interactions are governed by theories of contact mechanics and more details of the simulation algorithm used here can be found elsewhere [34].

Here we focused our attention on understanding the fabric anisotropy of the inclusion, for different cases of its size ratio. The force transmission characteristics of particulate assemblies are highly sensitive to the local arrangements of particles. Due to the strong dependence on particle arrangement, contact forces will usually be distributed in a complex, non-uniform manner [5]. The load is transmitted by relatively rigid, heavily stressed chains of particles which form a relatively sparse network of *strong contacts*, carrying greater than average normal contact force  $N$  ( $f = N / \langle N \rangle$ , and  $f > 1$ ). The remaining groups of particles, which separate the strong force chains, are referred to as *weak contacts*, and are only lightly loaded ( $f < 1$ ). Previous studies on the mechanics and physics of granular systems [2,4,5] indicate that the deviator stress in an assembly is produced by the dominantly strong contact network, forming a solid-like back bone structure while the weak force networks bear the

hydrostatic stress (fluid-like behaviour). The sliding of contacts dominantly occurs at these weak contact networks. Inspired by these findings, we analysed for the deviator fabric anisotropy of different classes of the contacts, viz., due to (i) all the contacts of the inclusion only ( $\phi_{i11}-\phi_{i33}$ ) and (ii) strong contacts of the inclusion ( $\phi_{is11}-\phi_{is33}$ ) under the external loading. The evolution of the fabric anisotropy of the contacts is measured using the well-known definition of the fabric tensor, suggested by Satake [33] as:  $\phi_{ij} = \langle n_i n_j \rangle = \frac{1}{M} \sum_{s=1}^M n_i^s n_j^s$ , where  $M$  is the number of contacts in the representative volume element and  $n^s$  is the direction of the  $s$ th branch vector.

At first, we present the nature of stress carried by the inclusions under the external loading. Figure 10 shows the evolution of the stress ratio of the inclusion, which is the ratio between the deviatoric stress of the inclusion ( $\tau_{Di}$ ) and the mean stress of the inclusion ( $p_s$ ). In this plot, we also provide an insert with stress ratio of the inclusions at steady state for different sizes of the inclusions. Form this plot, it is clear that, as concluded earlier from the experimental part, relatively large inclusions tend to carry less shear stress, thus more dominantly the nature of the stress is hydrostatic as reported earlier [20]. However, here we look for clues why this happens. To answer this, it would be interesting to study the variation of the fabric anisotropy of the inclusions during external loading.

In Fig.11, we examine in detail the fabric anisotropy of the inclusion for the two most important size ratio 5 and 10 in terms of its deviator fabric ( $\phi_{i11}-\phi_{i33}$ , suffix  $i$  denotes the inclusion). The inclusion size ratio of 10 is considered as important as we observed earlier that, for the size ratio of the inclusion greater than 10, the deviatoric stress ratio of the inclusion remained as almost constant. Here, we partition the fabric anisotropy of the

inclusion contributed by the strong ( $f > 1$ ) and weak contacts ( $f < 1$ ). It can be seen that, the fabric anisotropy of the inclusion contributed by the weak contacts is relatively independent of the size of the inclusion, whereas, the contribution to this due to the strong contacts is influenced by its size ratio. An increase in the size ratio of the inclusion decreases the fabric anisotropy of the strong contacts of the inclusion. This result, in combination with the outcomes of Fig.10, supports that the microscopic origin of shear stress mobilization of the inclusions is mostly due to their strong contacts. To emphasise this point, we also present the fabric deviator stress due to the strong contacts and the macroscopic deviator (shear) stress of the assemblies below.

For this, the structural anisotropy tensor  $\phi_{ij}$  can be decomposed as follows [34]:

$$\phi_{ij} = (1-v) \phi_{ij}^w + v \phi_{ij}^s \quad (1)$$

where the superscripts 'w' and 's' indicate the weak and strong force sub- networks and 'v' is the proportion of strong contacts. In order to examine the contribution of the sub network of contacts, the fabric stress  $\sigma_f$  can be defined as [33]:

$$\sigma_f = \sigma_{kk} \phi_{ij} \quad (2)$$

Figure 12 shows the variation between the macroscopic deviator stress ( $\sigma_{11} - \sigma_{33}$ ) and the fabric stress due to contacts carrying forces greater than average normal force, ie.,  $\sigma_{f\text{-strong}} = \sigma_{kk} \cdot (\phi_{11} - \phi_{33})_s$ , the suffix s denotes the strong contacts. It is evident that, macroscopic deviator stress levels agree fairly well with the corresponding fabric deviator stress due to the strong contacts. Though such a correlation is reported earlier [33], the present study shows that the fabric stress due to strong contacts (and bulk deviator stress) decreases for an increase in the size ratio of the inclusion. Hence we conclude that, increase in the size of the

inclusion tends to decrease their ability to mobile shear here. This is also observed from the photo stress experiments reported earlier for inclusions when positioned away from the wall boundaries. This is due to: increase in the size of the inclusion tends to decrease its fabric anisotropy, in particular, the fabric anisotropy of the strong contacts of the inclusions under the external loading. To conclude, the presence of the inclusion tends to retard its ability to establish a strongly anisotropic fabric structure and hence reduces its ability to sustain shear especially away from the wall boundary.

## **5. Conclusions**

By studying the optical response of the inclusions inside granular assemblies under axial compression, we have provided new insights on the nature of stress experienced by the inclusions of different sizes in relation to their distance from the wall boundary. Depending on the proximity of inclusions to the wall, they display different levels of shear sustaining ability. Inclusions of all sizes sustain a high level of shear close to the wall boundaries. However, this intensity drops in the large size inclusions when they reside away (more than about 4 times their size) from the wall boundary. Away from the wall boundary, the big particles experience significantly less shear stress (and conversely tend towards hydrostatic state) as displayed by the distribution of the maximum shears stress and the direction of major principal stress within the inclusions. Using DEM simulations, we investigated the average nature of stress experienced by large inclusions (three-dimensional) under periodic boundary conditions and, subjected to tri-axial compression. These results are in qualitative agreement with the experimental research reported earlier. The increase in the size of the inclusions decreases the tendency of the particles to sustain shear stress inside particulate packing. Using simulations, we studied the fabric anisotropy of the contacts supporting the

inclusions inside the particulate systems under external loading. We found that the drop in the shear state of the large inclusions, especially away from the wall boundaries, could be attributed to their fabric anisotropy of strong contacts. This decreases for an increase in the size ratio of the inclusion. Based on this study, we suggest that it would be more appropriate to revisit the constitutive relations and failure criteria employed in advanced simulation methodologies, where single-particle scale information is assessed. For example in DEM, variations in the stress distributions *within* the particles is often ignored (independent of particle size) and usually shear failure strength of particles are prescribed to occur at inter-particle contacts, independent of their size and wall effects. In future, efforts should be made to include more realistic descriptions of grain-scale constitutive behaviour depending on their size and, proximity to wall boundaries, for understanding their micromechanical behaviour. The present study is not without any limitations. For example, in future combined FEM-DEM simulations are to be performed to computationally map out the *local distribution* of shear stress within three dimensional inclusions more rigorously rather than its average measures using contact forces (acting at the boundary of the inclusion) in the DEM simulations reported here. Further detailed studies are required to account for variables such as the roughness effects of the wall boundaries, different packing densities, distribution of particle sizes and multi-axial loading conditions.

## References

1. W.R Ketterhagen *et al.*, Process Modeling in the Pharmaceutical Industry using the Discrete Element Method, *Jl. Phar. Sci.* 98(2) (2009) 442-470
2. F. Radjai *et al.*, Force distributions in dense two-dimensional granular packing, *Phys. Rev. Lett.* 77(2) (1997) 274-277
3. D. Muehth *et al.*, Contact force measurements and stress-induced anisotropy in granular materials, *Nature.* 406 (2000) 385-389
4. N.P. Krut and S.J. Antony, Force, relative displacement and work networks in granular media subjected to quasi-static deformation, *Phys. Rev. E.* 75 (2007) 051308

5. S.J. Antony, Link between single-particle properties and macroscopic properties in particulate assemblies: role of structures within structures, *Phil. Trans. Roy. Soc. Lond. A.* 365 (2007) 2879-2891
6. A. Drescher and de J. Jong, Photoelastic verification of a mechanical model for the flow of a granular material, *Jl. Mech. Phys. Sol.*, 20 (1972) 337-351
7. D. Howell and R.P. Behringer, Stress fluctuations in a 2D granular couette experiment: A continuous transition, *Phys. Rev. Lett.* 82(26) (1999) 5241-5244
8. S.J. Antony and D. Chapman, Probing shear stress distribution within single particle scale inside particulate packing, *KONA Powd. Part. Jl.* 28 (2010) 180-188
9. S.J. Antony, O. Imafidon and T. Barakat, Micromechanical analysis of inclusions in particulate media using digital photo stress analysis tomography, *Opt. Eng.* 54(8) (2015) 081202
10. P.A. Cundall and O.D.L. Strack, A discrete numerical model for granular assemblies, *Geotech.* 29(1) (1979) 47-65
11. A. Munjiza, *The combined finite-discrete element methods*, Wiley, Chichester, 2004
12. H.G. Matuttis et al., Discrete element methods for the simulation of dense packings and heaps made of spherical and non-spherical particles, *Powder Tech.* 109 (2000) 278-292
13. H.P. Zhu, Z.Y. Zhou, R.Y. Yang and A.B. Yu, Discrete particle simulation of particulate systems: A review of major applications and findings. *Chem. Eng. Sci.* 63 (2008)5728–5770
14. M. Quintanilla et al., Correlation between bulk stresses and interparticle contact forces in fine powders. *Phy. Rev. E.* 64 (2001) 031301
15. S.J. Antony and M.A. Sultan, Evolution of the invariants of stress and fabric tensors in granular systems subjected to electro-mechanical loading. *Mech. Mat.* 41(6) (2009) 742-747
16. S.J. Antony and M.A. Sultan, Role of inter-particle forces and inter-particle friction on the bulk friction in charged granular media subjected to shearing. *Phy. Rev. E.* 75(1) (2007) 031307
17. D.M. Walker and A. Tordesillas, Mesoscale and macroscale kinetic energy fluxes from granular fabric evolution, *Phy. Rev. E.* 89 (2014) 032205
18. A. Almaya and A. Aburub, Effect of particle size on compaction of materials with different deformation mechanisms with and without lubricants, *AAPS Pharm.Sci.Tech.* 9(2) (2008) 414-418
19. G.R. McDowell and M.D. Bolton, On the micromechanics of crushable aggregates, *Geotech.* 48(5) (1998) 667–679
20. S.J. Antony and M. Ghadiri, Size effects in a slowly sheared granular media. *Jl. App. Mech.* 68(5) (2001) 772-775
21. M.R. Kuhn and K. Bagi, Specimen size effect in discrete element simulations of granular assemblies, *Jl. Eng. Mech.* 135(6) (2009) 485-492
22. C.-Y.Wu et al., Modelling the mechanical behaviour of pharmaceutical powders during compaction, *Powd. Tech.* 152 (2005) 107–117
23. S-Y.Fu et al, Effects of particle size, particle/matrix interface adhesion and particle loading on mechanical properties of particulate–polymer composites. *Comp. B.* 39 (2008) 933–961
24. A. Drescher and G. de-Josselin-de-Jong, Photoelastic verification of a mechanical model for the flow of a granular material. *Jl. Mech. Phys. Sol.* 20 (1972) 337–351
25. J.W. Dally and W.F. Riley, *Experimental stress analysis*, McGraw Hill, Singapore, 1987
26. O. Tsoungui, D. Vallet, and J.C. Charmet, Numerical model of crushing of grains inside two-dimensional granular materials, *Powd. Tech.* 105 (1999) 190–198

27. A. Hassanpour, S.J. Antony and M. Ghadiri, Modelling of agglomerate behaviour under shear deformation: Effect of velocity field in high shear mixer granulator on the structure of agglomerates, *Adv. Powd. Tech.* 18(6) (2007) 803-811
28. V.M. Kenkre, M.R. Endicott, S.J. Glass and A.J. Hurd, A theoretical model for compaction of granular materials. *Jl. Am. Cer. Soc.* 79(12) (1996) 3045-3052
29. D. Kolymbas, *Constitutive modelling of granular materials*, Springer-Verlag, Berlin Heidelberg, 2000
30. K.L. Johnson, *Contact mechanics*, Camb. Uni. Press, Cambridge, 2003
31. S.J. Antony, Evolution of force distribution in three dimensional granular media, *Phy. Rev. E.* 63(1) (2001) 011302
32. M.M. Mehrabadi, B. Lorent and S. Nemat-Nasser, Incremental constitutive relations for granular materials based on micromechanics. *Proc. Roy. Soc. Lond. A.* 441 (1993) 433-463
33. C. Thornton, Numerical simulations of deviatoric shear deformation of granular media. *Géotechnique*, 50(1), 43 –53 (2000)
34. Thornton, C., and Antony, S.J. Quasi-static deformation of particulate media. *Phil. Trans. Roy. Soc. Lond. A.* 356(1747) (1998) 2763-2782
35. M. Satake, Fabric tensor in granular materials, in P.A. Vermeer and H.J. Luger (eds.), *Deformation and Failure of Granular Materials*, Balkema, Rotterdam, 63-68, 1982
36. M. Oda, S. Nemat-Nasser and M.M. Mehrabadi, A statistical study of fabric in a random assembly of spherical granules, *Intl. Jl. Num. Anal. Meth. Geom.* 6 (1982) 77-94
37. M.M. Mehrabadi, S. Nemat-Nasser and M. Oda, On statistical description of stress and fabric in granular Materials. *Intl. Jl. Num. Anal. Meth. Geom.* 6 (1982) 95-108
38. G. Subhash, S. Nemat-Nasser, M.M. Mehrabadi and H.M. Shodja, Experimental investigation of fabric-stress relations in granular materials, *Mech. Mat.* 11(2) (1991) 87-106
39. J. Konishi, M. Oda and S. Nemat-Nasser, Induced anisotropy in assemblies of oval cross-sectional rods in biaxial compression, in J.T. Jenkins and M. Satake (eds.), *Mechanics of Granular Materials: New Models and Constitutive Relations*, Proc. U.S.-Jap. Semi., Ithaca, NY, Elsevier, 31-39, 1983
40. J. Zhang, T.S. Majmudar, A. Tordesillas and R.P. Behringer, Statistical properties of a 2D granular material subjected to cyclic shear, *Gran. Matt.* 12(2) (2010) 159-172
41. S. Nemat-Nasser and M.M. Mehrabadi, Micromechanically based rate constitutive descriptions for granular materials, in C.S. Desai and R.H. Gallagher (eds.), *Mech. Eng. Mat.*, John Wiley and Sons 451-463, 1984
42. S. Nemat-Nasser, A micro mechanically-based constitutive model for frictional deformation of granular materials. *Jl. Mech. Phy. Sol.* 48 (2000), 1541-1563
43. M.M. Mehrabadi and S. Nemat-Nasser, Stress, dilatancy and fabric in granular Materials, *Mech. Mat.*, 2(2) (1983) 155-161

#### ACKNOWLEDGEMENT

This Project was funded by the National Plan for Science, Technology and Innovation (MAARIFAH), King Abdulaziz City for Science and Technology, Kingdom of Saudi Arabia, Award Number (11-NAN-1877-02).

## Figure captions:

Fig.1: (a) Illustration of the granular bed with inclusion subjected to axial compression. Different sizes of the inclusion were considered in this study. The effects of proximity of the wall boundaries on inclusion are examined for different values of  $\lambda d$  and (b) Schematic diagram of PSAT set up [8,25].

Fig.2: Distribution of maximum shear stress within the inclusion for the case of inclusion in contact with the wall ( $\lambda=0$ ) and for typical cases of loading (P). The direction of major principal stress distribution (small arrows) is also superimposed on these plots. For ease, the double-headed guiding arrows show the most dominant direction of major principal stress direction in the inclusions.

Fig.3: Maximum shear stress distribution displayed by the biggest inclusion (size ratio 7) at different proximities from the wall position (varying  $\lambda$ ). The direction of major principal stress distribution (small arrows) is also superimposed on these plots. For ease, the double-headed guide arrows illustrate the dominant direction of the major principal stress in the inclusions. The stress levels are colour coded using the same scaling as shown in Fig.2.

Fig.4: Illustration of the scanning lines to examine the variation of maximum shear stress ( $\tau_{max}$ ) within an inclusion. 2a represents the contact width of a typical neighbouring grain in contact with the inclusion. The starting point of the scan line (represented in red circles on the insert) is the closest contact point to the positions of  $\theta=0, 45, 90$  and  $135$  degrees and ends at the opposite mirror image points.

Fig.5: Typical distribution of the maximum shear stress experienced by the lowest and largest inclusions studied here in contact with the wall ( $\lambda=0$ )

Fig.6: Distribution of the maximum shear stress experienced by the inclusion with size ratio 2.5 for different proximities to the wall

Fig.7: Distribution of the maximum shear stress (MPa) experienced by the inclusion with size ratio 7 for different proximities to the wall

Fig.8: Value of  $Z_{max}$  of the inclusions under different load levels ( $\lambda=0$ )

Fig.9: Schematic diagram of the cross section of a periodic cell with an inclusion (larger particle) at the middle, surrounded by smaller particles under an external loading

Fig.10: Stress ratio of the inclusion under the mechanical loading. The insert shows the stress ratio at steady state for different sizes of the inclusion.

Fig.11: Fabric anisotropy of selected cases of the inclusion under external loading. They are partitioned based on the contribution of their strong and weak contacts

Fig.12: Variation of fabric deviator stress due to strong contacts and macroscopic deviator stress

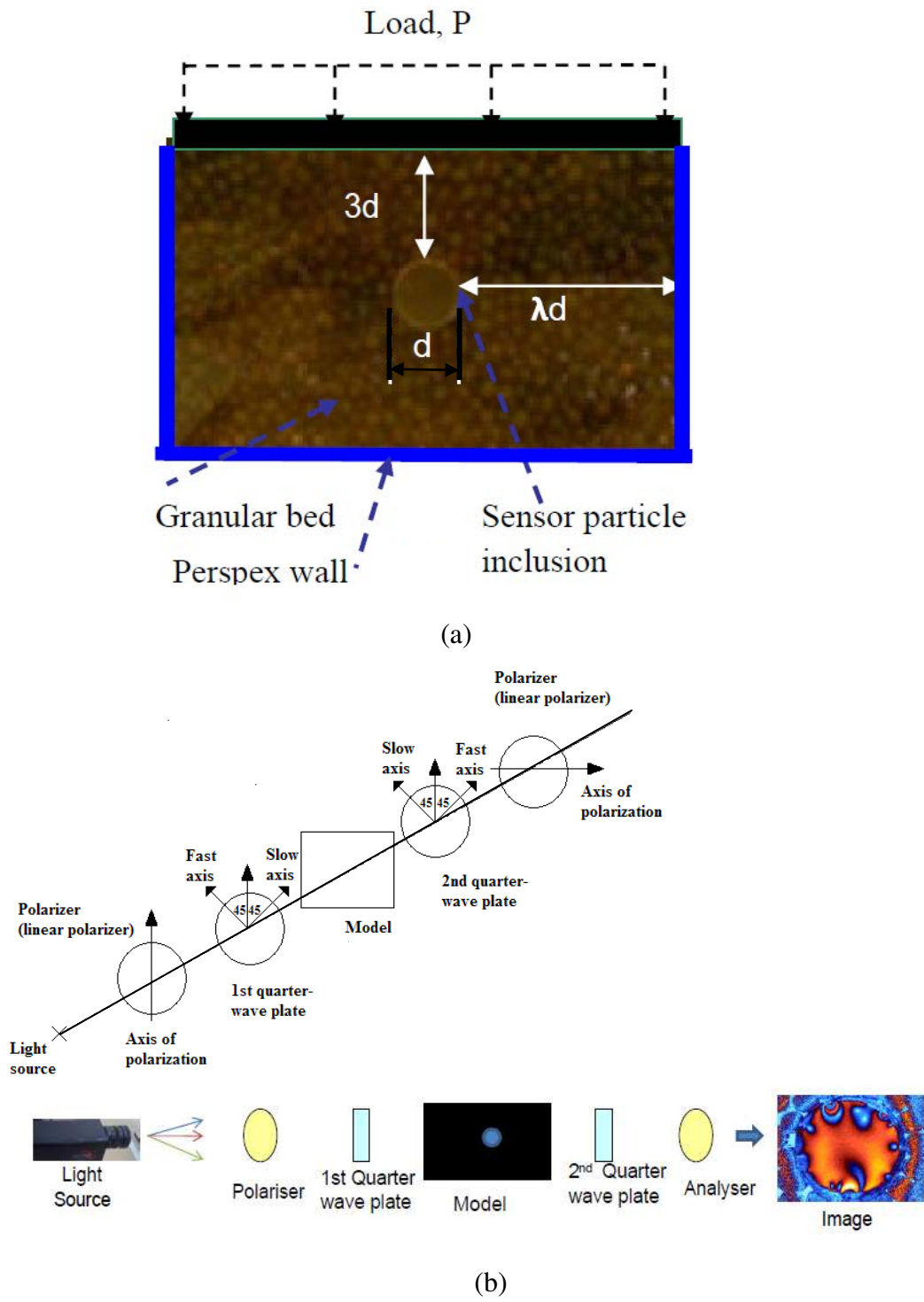
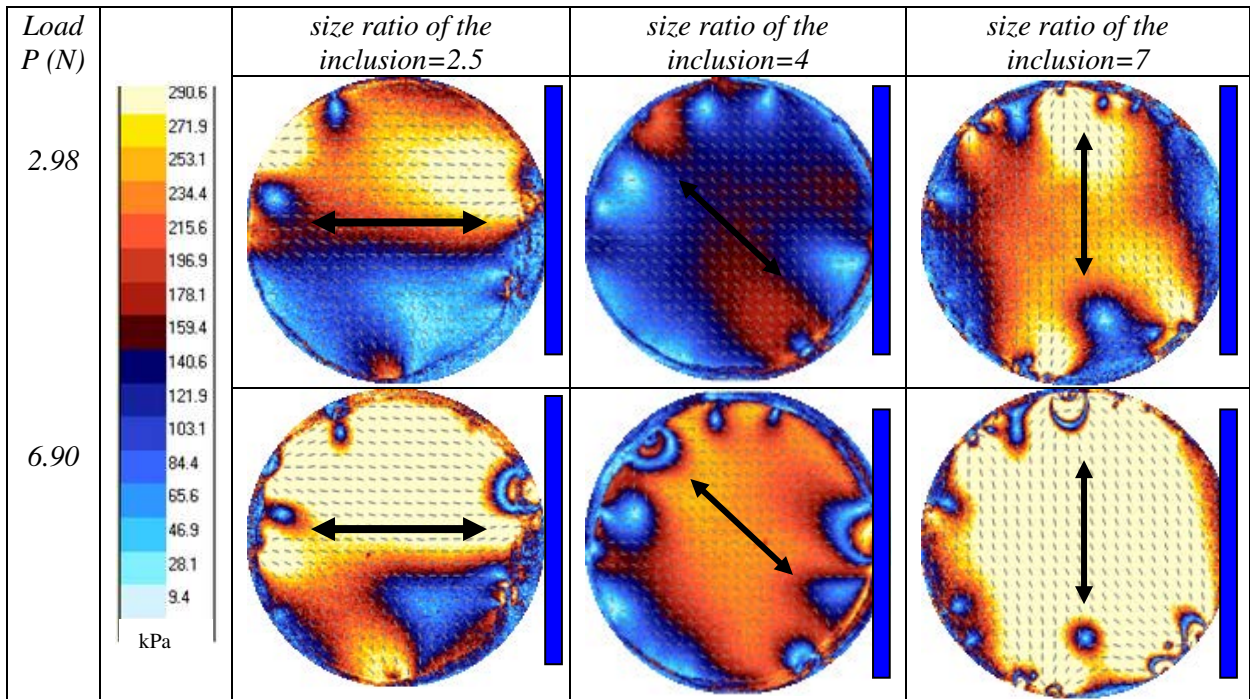
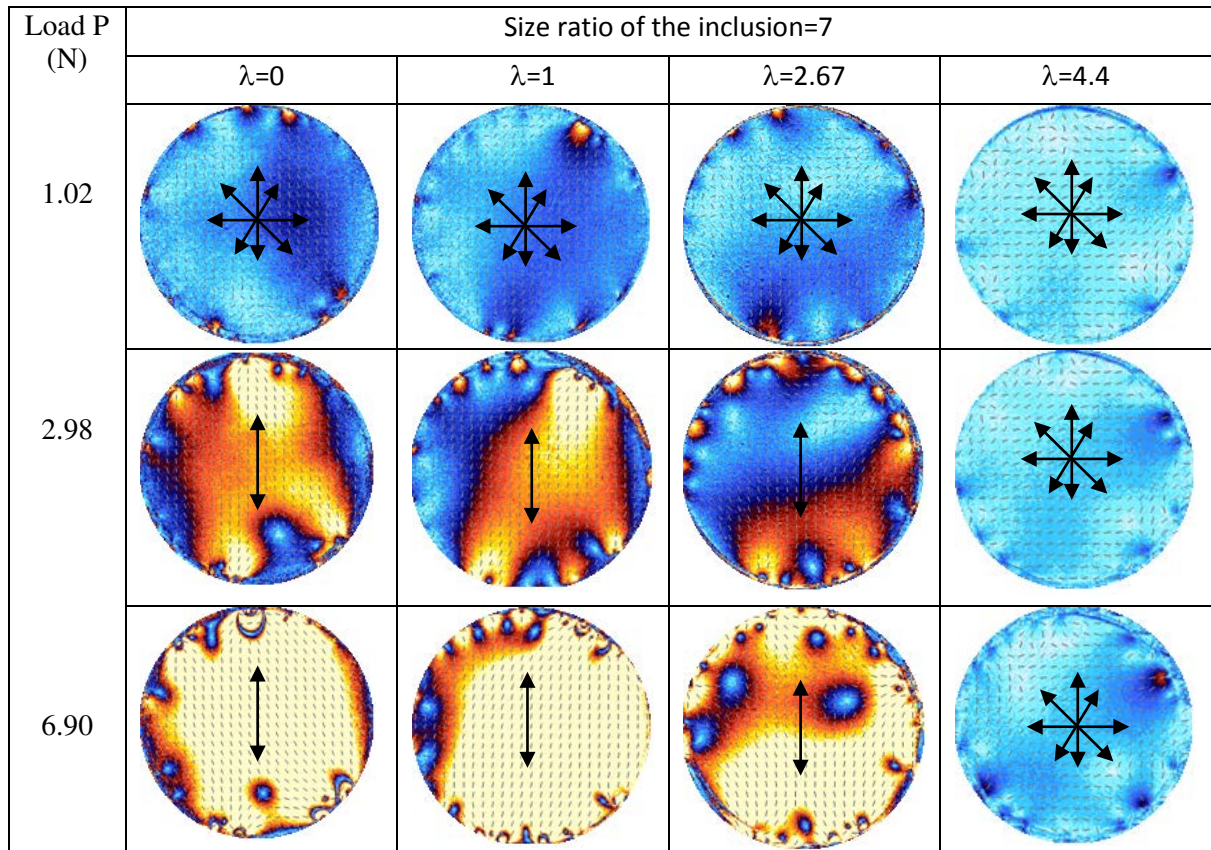


Fig.1



**Fig.2**



**Fig.3**

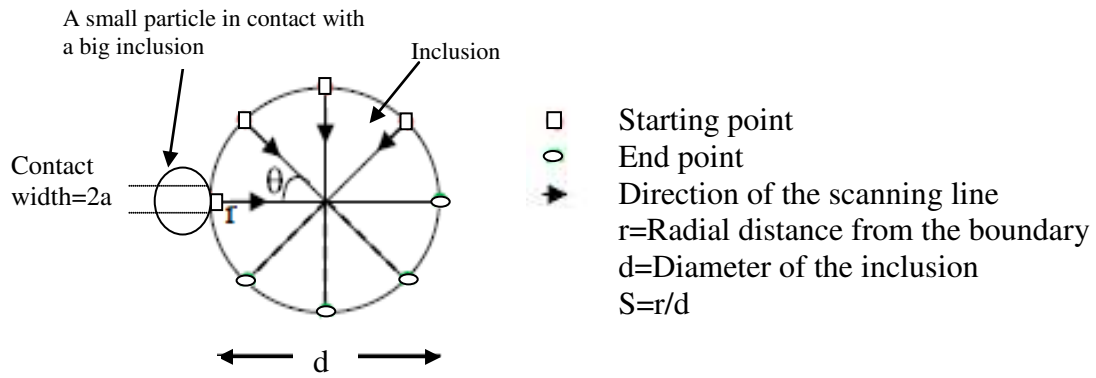


**Fig.4**

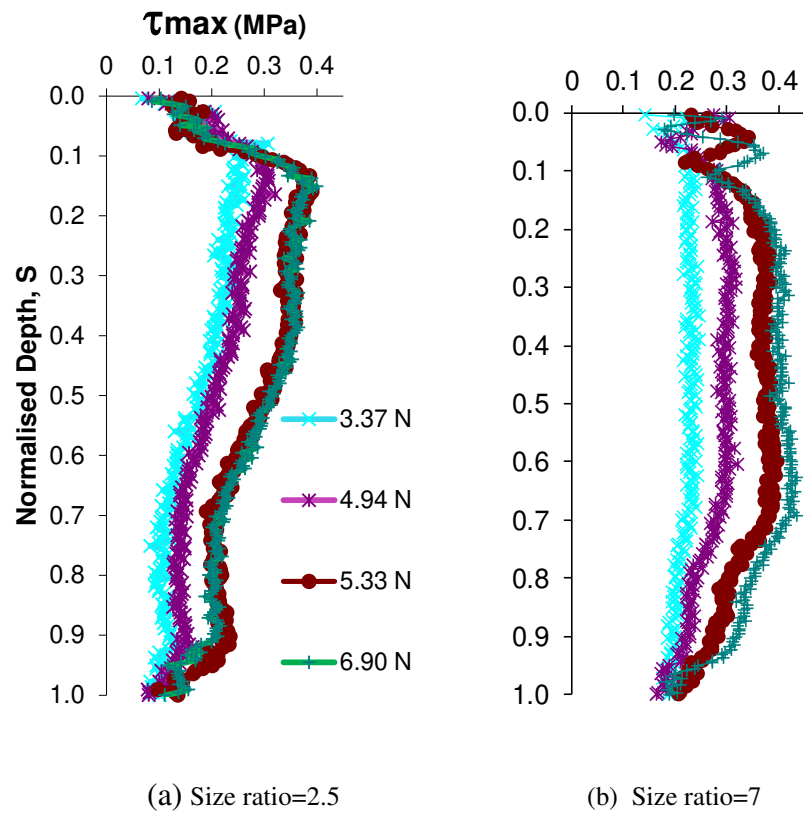


**Fig.5**

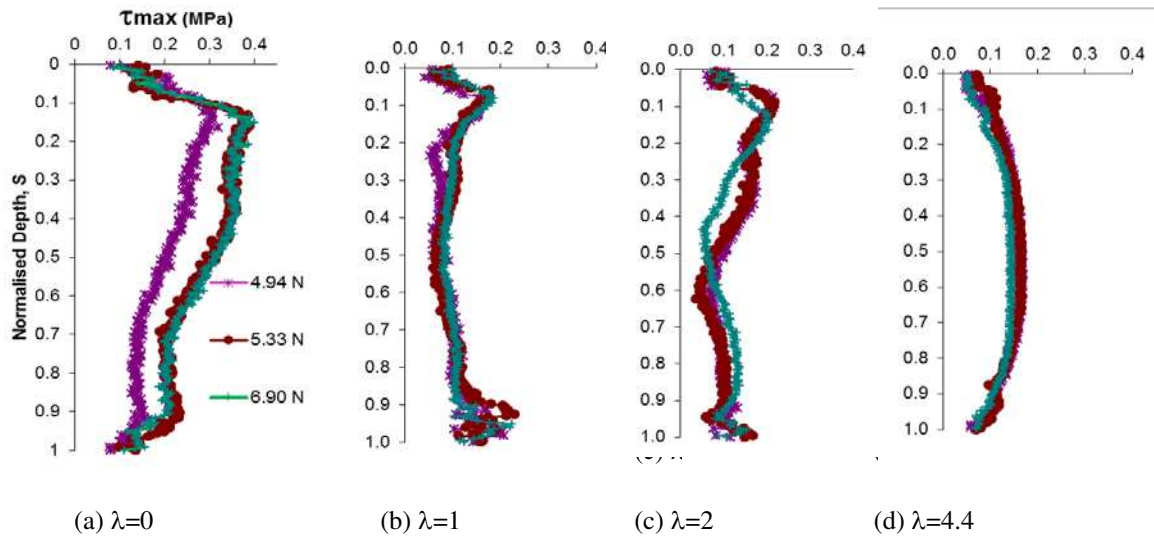


**Fig.6**

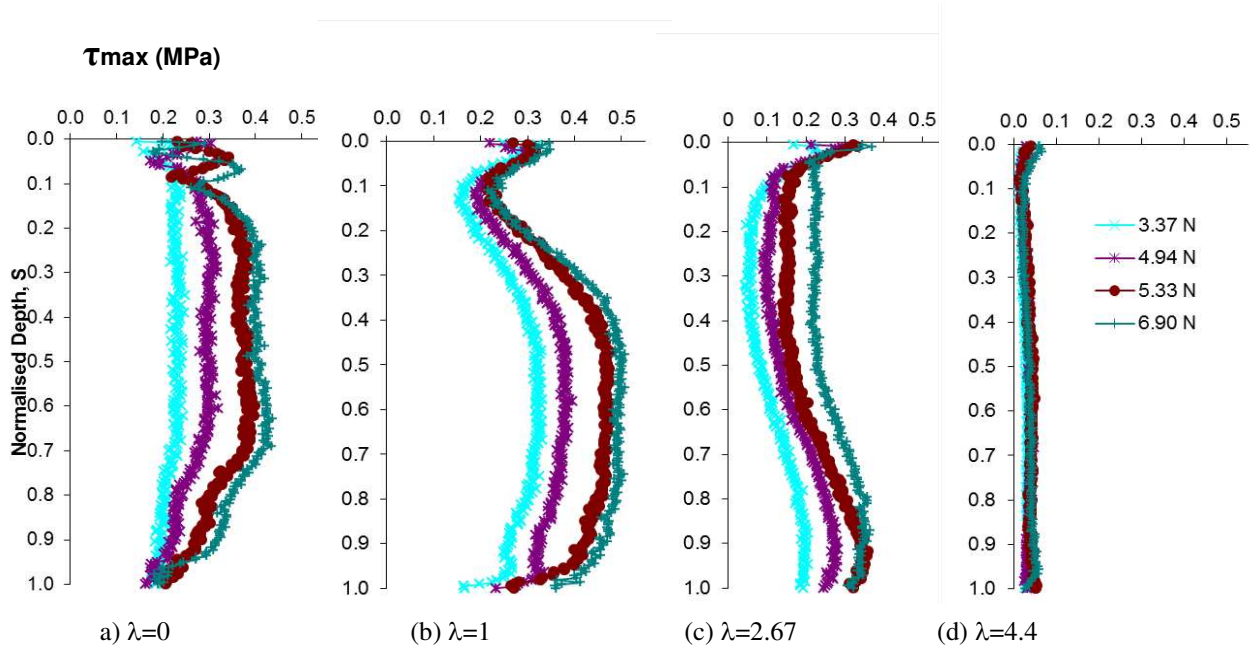


**Fig.7**

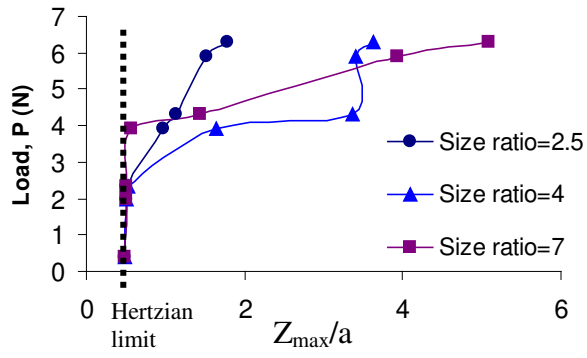


Fig.8

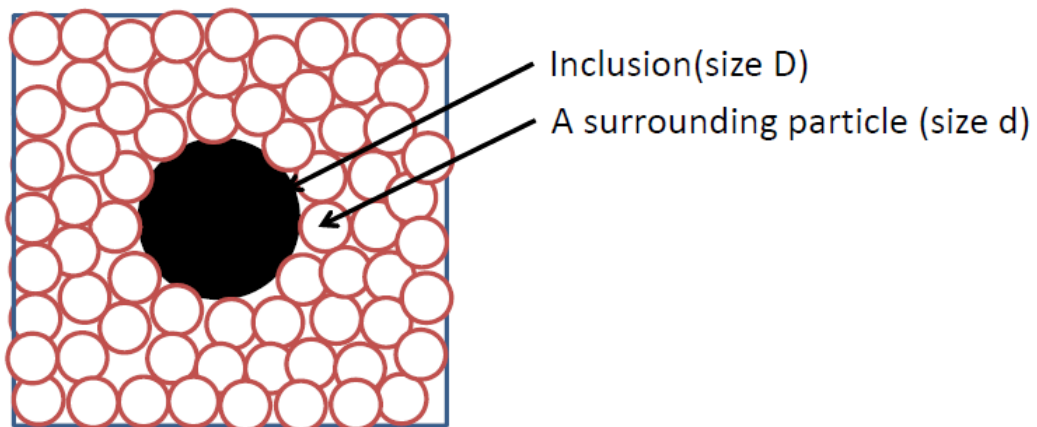
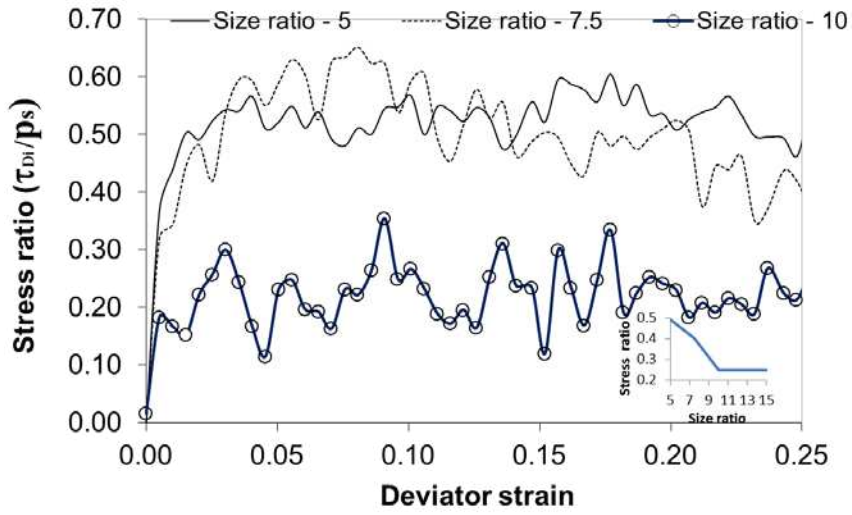
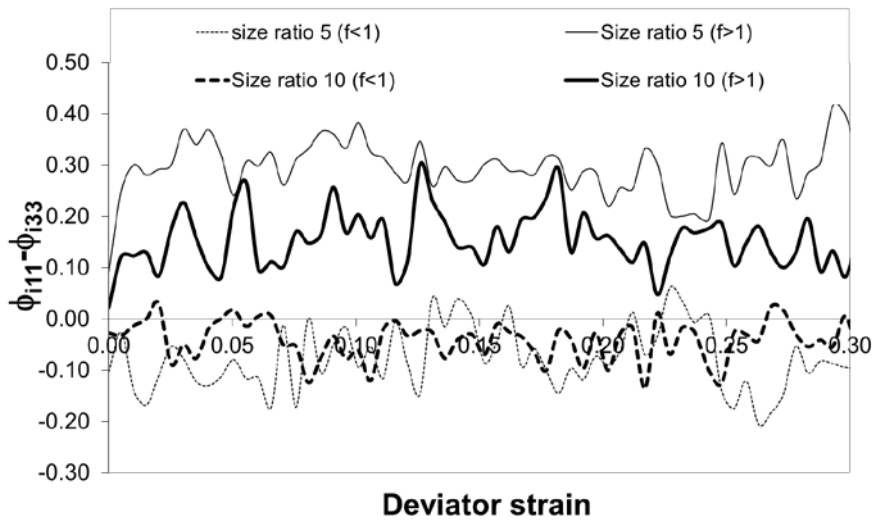


Fig.9



**Fig.10**



**Fig.11**

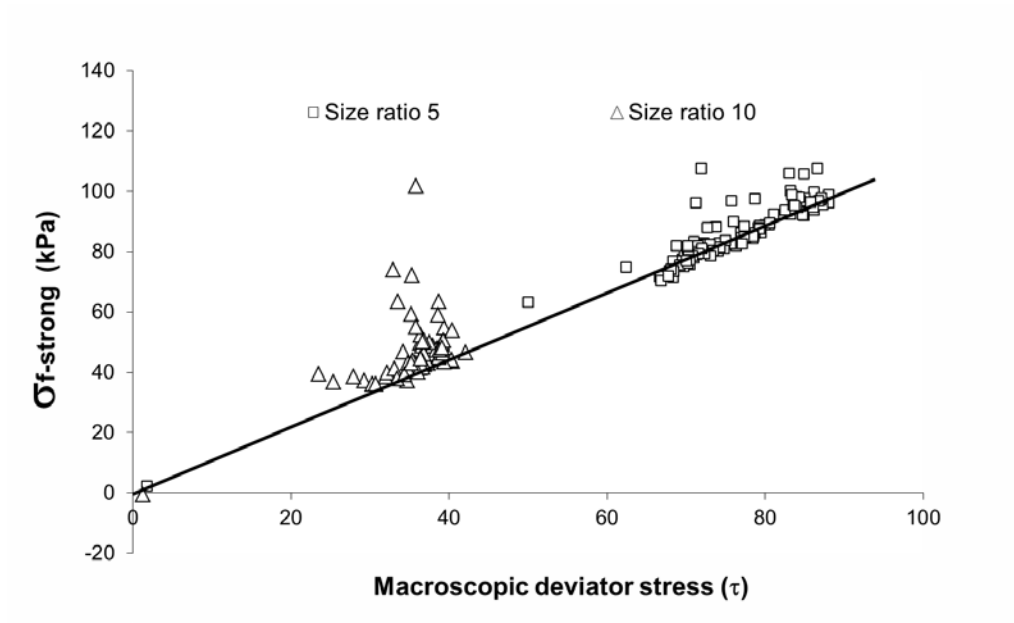


**Fig.12**

## Highlights:

- Relatively large inclusions experience strong shear close to the wall boundaries
- Away from the wall, the above said nature of stress tends to be hydrostatic
- Smaller size inclusions could experience shear, close to and away from the wall
- Qualitatively, the DEM simulation results agree with the PSAT experiments
- Microscopic origin of shear in the inclusion is attributed to its fabric anisotropy

## Graphical Abstract:

